

Bionanocomposites of PLA/PBAT/organophilic clay: preparation and characterization

Josiane Dantas Viana Barbosa¹ , Joyce Batista Azevedo², Edcleide Maria Araújo³,
Bruna Aparecida Souza Machado^{1*} , Katharine Valéria Saraiva Hodel¹ and Tomas Jefferson Alves de Mélo³

¹*Laboratório de Formulações Farmacêuticas, Instituto de Tecnologias da Saúde (ITS),
Centro Universitário SENAI CIMATEC, Salvador, BA, Brasil*

²*Departamento de Materiais, Universidade Federal do Recôncavo da Bahia – UFRB,
Feira de Santana, BA, Brasil*

³*Departamento de Materiais, Universidade Federal de Campina Grande –
UFCG, Campina Grande, PA, Brasil*

*brunam@fiieb.org.br

Abstract

The objective of this study was to develop bionanocomposites from blends of poly(lactic acid) (PLA) and poly(butylene adipate-co-terephthalate) (PBAT) and from 3% and 6% bentonite clay. Initially, the bentonite clay was treated with Praepagen salt, and the properties of the modified clay were evaluated. After the organophilization of the clay was completed, 50:50 blends of PLA/PBAT were prepared, and 3 and 6% clay was added. To test the dispersion of the system, the blending sequence was performed using eight different sequences for the addition of clay to the PLA/PBAT matrices. The mixtures were prepared in a twin screw extruder, and the specimens were subsequently injection molded. The investigated mechanical and morphological properties included the yield strength, yield strain, tensile and bending elastic modulus, and scanning and transmission electron microscopy analyses. The results of this study showed increases of the mechanical properties when nanoparticles were added and the formation of bionanocomposites with intercalated structures.

Keywords: *bionanocomposite, nanoclay, PBAT, PLA, bionanocomposites.*

How to cite: Barbosa, J. D. V., Azevedo, J. B., Araújo, E. M., Machado, B. A. S., Hodel, K. V. S., & Mélo, T. J. A. (2019). Bionanocomposites of PLA/PBAT/organophilic clay: preparation and characterization. *Polímeros: Ciência e Tecnologia*, 29(3), e2019045. <https://doi.org/10.1590/0104-1428.09018>

1. Introduction

In the last 50 years, polymers derived from petroleum have been used extensively due to their versatility, mechanical properties, and relatively low cost. However, its extensive use has had environmental impacts because a large volume of waste is disposed of in the environment, especially disposable plastics packaging^[1,2]. As a result, plastic packaging has become one of the main contributors to the various environmental impacts since over a third of current plastics production is used to make them, and also because its relatively short life cycle^[3,4]. In addition, recent increases in the cost of raw petroleum have led to a dramatic increase in the cost of plastics. Technologies for recovering plastic have also improved in recent years but are not totally free from environmental damage^[5].

As a result, society has pressured the industrial sector to adopt innovative environmentally friendly policies, such as the rational use of natural resources, especially in the production of resins for the productive sector. In this context, several materials have been researched in the search for environmentally favorable solutions^[6-10]. As an alternative to reduce environmental impacts, a new class of materials,

biopolymers, has emerged and have motivated a significant number of studies due to the large environmental interest and possible lack of fossil resources^[2,11-15].

Compared to conventional thermoplastics, biopolymers exhibit poor performance in several specific properties and therefore must be modified to become more competitive^[16-19]. This process resulted in different biopolymers with smart behavior and a significant change in one property upon an external trigger^[20]. Biodegradable polymers are not easily classified because they can be organized according to their chemical composition, synthesis method, processing method, economic relevance, and application^[21-27].

These biopolymers are commonly blending with other biopolymers or with conventional polymers and/or inorganic particles. The blending of biopolymers with other polymers provides a way to modify the properties of biopolymers and can reduce the overall cost of the material. These blends form a new class of materials: biocomposites that are obtained from based on biodegradable polymers as matrix^[6,28-30]. Poly(lactic acid) (PLA) and poly(butylene adipate-co-terephthalate) (PBAT) are among the polymers

most investigated as possible matrices for the formation of these blends, on account of chemical and mechanical properties, besides being both biodegradables^[30-32].

The development of polymer blends using nanotechnology has emerged as a possible solution that may be adopted in different fields of technology to improve mechanical, barrier, flammability, thermal, electric, and cosmetic properties^[33-35]. Nanoclay is among the most studied nanomaterials, because its potential of use is variable fields, thanks to properties such as the highly oriented nanoclay structures showed a tortuous path that was responsible for the reduced gas and vapor transmission^[36]. Besides that, nanoclay provides increased of the nanocomposite tensile strength and the compressive, fracture and Young's modulus were related to the dispersion of the clay, degree of delamination, form factor of the clay, and polymer-clay interfacial interactions^[37-40]. Correa et al.^[15] and Kumar et al.^[41] analyzed the properties of Polyhydroxybutyrate/Polycaprolactone (PHB/PCL) and PLA/PBAT blends, respectively, incorporated with nanoclays. The results showed that the blends with the nanoclays presented better thermal stability, mechanical, and barrier properties when compared to their respective controls.

In this context, the aim of this study was to develop bionanocomposites from two polymer matrices, PLA and PBAT with bentonite clay, using the melt intercalation technique with different blending sequences and to then evaluate the mechanical and morphological properties of the bionanocomposites obtained.

2. Materials and Methods

2.1 Materials

Brasgel PA clay, supplied by Indústria Bentonit União Nordeste (BUN), located in Campina Grande, Paraíba, Brazil, was used to obtain organophilic clay. Industrialized clay was treated with Praepagen WB® salt and the following procedure was adopted: dispersions containing 768 mL of distilled water and 32.0 g of clay were prepared. The clay was slowly added with concomitant mechanical stirring and after the addition of all the clay the stirring was maintained for 20 minutes. Then, a solution containing 20 mL of distilled water and 20.4 g of the quaternary ammonium salt was added. Stirring was continued for another 20 minutes. Sequentially, the containers were closed and kept at room temperature for 24 h. After that, the material obtained was washed and filtered to remove excess salt. The washing was done with 2000 mL of distilled water, using Buchner Funnel with kitassato, coupled to a vacuum pump with a pressure of 635 mmHg. The agglomerates obtained were oven dried at 60 °C ± 5 °C for a period of 48 h. Finally, the dry agglomerates were disaggregated with the aid of a mortar until powdery materials were obtained, which were passed in ABNT No. 200 sieve for further characterization.

Two polymers were used as polymer matrices: i) poly(lactic acid) (PLA), which was supplied by Cargill-Dow and is commercially known as Nature Works 2002D and ii) poly(butylene adipate-co-terephthalate) (PBAT), a biodegradable polyester that was supplied by BASF and is commercially known as ECOFLEX® F BX 7011.

2.2 Preparation of the PLA/PBAT/Clay (OMMT) systems

Eight PLA/PBAT blend samples with 50/50 weight ratios that contained clay at concentrations of 3% and 6% were investigated. These polymer/clay systems were prepared in a modular co-rotating twin screw extruder (model DRC 30:40 IF, Imacom, Barretos, Brazil) with a thread diameter of 30 mm and an L/D ratio of 30 that was fitted with a degassing system. Before processing, the organophilic clay and the polymer matrices were dried at 100 ± 5 °C for three hours in a forced air oven. First, the materials were weighed and pre-blended by tumbling. The samples were subsequently dosed at the main feed zone of the extruder (beginning of the thread) using a volume doser from Brabender.

To investigate the influence of the blending sequence of the material, four procedures were used to obtain 50% PLA and 50% PBAT blends for both clay concentrations (3% and 6%) as described: (1) For the first blending sequence, a blend of 50% PLA and 50% PBAT was prepared with the extrusion technique, and 3% and 6% by weight of clay was then added to the PLA/PBAT blend, which was extruded again; (2) For the second sequence, concentrates that contained PBAT and 3% and 6% by weight of clay were prepared by the extrusion technique, and PLA was then added to the systems with the extrusion technique; (3) For the third sequence, concentrates that contained PLA and 3% and 6% by weight of clay were prepared with the extrusion technique, and PBAT was then added to the systems with the extrusion technique; and, (4) For the fourth sequence, the three components (PLA/PBAT/clay) were added simultaneously with 3% and 6% concentrations by weight of clay and processed using the extrusion technique.

The temperatures in the 10 zones in the twin screw extruder for the PLA and PBAT blends were Z1 = 140 °C, Z2 = 150 °C, Z3 = 175 °C, Z4 = 180 °C, Z5 = 185 °C, Z6 = 185 °C, Z7 = 185 °C, Z8 = 175 °C, Z9 = 175 °C and Z10 = 170 °C^[42]. A screw speed of 80 rpm was used for the 3% (PLA + clay) and (PBAT + clay) concentrations, and 60 rpm was used for the 6% clay concentrations. The measured temperature of the molten polymer was 185 °C, and the same screw configuration was used for all the investigated samples^[43]. The extruded material was granulated and dried, and the injected specimens were subsequently prepared as will be described throughout the text. The thread profile is illustrated in Figure 1.

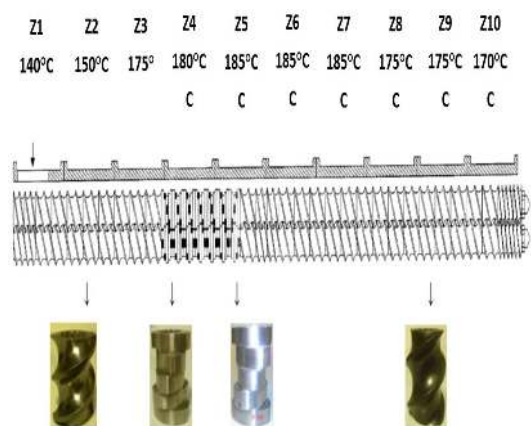


Figure 1. Thread profile used for processing the PLA/PBAT/clay systems (Redrawn from Ref.^[44]).

First, the blends described above were dried for 4 h at 50 °C. Specimens were then produced using the injection molding process. The samples were prepared in injection machine with a mold clamping force of 100 tons, manufactured by ROMI model PRIMAX 120 (Santa Bárbara d'Oste, Brazil). The injection conditions were: injection pressure of 250 bar, injection velocity of 120cm³/s, settling of 1s / 100 bar and tube temperature profile of T1 = 170 °C, T2 = 170 °C T3 = 175 °C and (no) nozzle T4 = 160 °C (injection nozzle). Samples were produced for tensile/bending strength and Izod impact strength tests according to standards ISO 527 and ISO 180.

2.3 Mechanical properties

Tensile/bending measurements were performed according to standard ISO 527 at a temperature of 25 ± 2 °C and a relative humidity of 55 ± 5%. Five specimens were tested on average for each sample. The tests were performed in an universal testing machine (model DL200, EMIC) at a constant speed of 10 mm/min. Notched Izod impact strength tests were performed according to standard ISO 180 on an EMIC impact tester.

2.4 X-ray diffraction

X-ray diffraction (XRD) analyses of the 8 samples were performed on a diffractometer (model XRD 6000, Shimadzu) that operated with copper K α radiation ($\lambda=1.5406$), 40 kV and 30 mA. Diffraction patterns were collected at a scanning rate of 20(2 θ)/min in the interval of 1.50<2 θ <300 with exposition the 60sec.

2.5 Scanning electron microscopy

Scanning electron microscopy (SEM) analyses of the 8 samples were performed on a microscope (model SSX-550, Shimadzu, Kyoto, Japan) that operated under different conditions, which can be observed in the captured images. The injected specimens underwent brittle fracture in liquid nitrogen, and the fracture surfaces were analyzed.

2.6 Transmission electron microscopy

For the transmission electron microscopy (TEM) analyses, samples were prepared by reducing the cross-sectional area of the sample ("trimming"), and the edge of the sample to be ultramicrotomed was sized into a trapezoidal shape for a

better stress distribution when cutting thin slices (sections) with a surface area of approximately 0.5 mm².

The samples were cut with an ultramicrotome (model Reichert Ultracut S, Leica) using a diamond knife (Diatome) at a cutting temperature of -40 °C under liquid nitrogen at a cutting speed of 0.1 mm.s⁻¹ and a slice thickness of 25 nm. The cryo-ultramicrotomed samples were observed in a TEM (model CM120, Philips) with a voltage of 120 kV.

3. Results and Discussions

3.1 Mechanical characterization

Table 1 presents the values obtained for the yield strength, yield strain, and tensile and bending elastic moduli for the PLA/PBAT blend and the PLA/PBAT/clay systems investigated. The maximum yield strength of the systems with clay was 24.3 MPa for sample 7 (PLA 6% clay concentrate + PBAT), and the minimum was 8.3 MPa for sample 6 (PLA 3% clay concentrate + PBAT). The maximum yield strain was 2.0% in sample 5, and the minimum yield strain was 1.0% in sample 6 (PLA 6% clay concentrate + PBAT). The results indicate that different blending conditions and the addition of different concentrations of clay cause changes in the mechanical properties. It is important to emphasize that this system is composed of two polymer matrices with distinct behaviors. Different studies with PLA/PBAT blends, showed the use additives to improve properties mechanical and morphology such as Signori et al.^[45] and Jiang et al.^[46]. These studies suggested that adding PBAT to the PLA matrix increased the ductility of the PLA.

In the other study, Ko et al.^[47] made PLA/PBAT blends and carbon nanotubes 2% (MNWT) in the presence the antioxidant additive. It has verified that the PLA/PBAT blends are immiscible, and that the MWNT has a (referential) affinity for the PBAT phase and this phenomenon makes unique morphological properties of the nanocomposite system. Such a strong affinity of the MWNT to the PBAT phase might be related to chemical structure of the PBAT which possesses aromatic molecules in its main chain, as many groups reported that MWNT prefers aromatic molecules. Therefore, having as reference these results, the increases in the properties resulted from the greater dispersion of the clay in the PLA/PBAT blend, which provided greater interaction between the two matrices and consequently improved the results.

Table 1. Mechanical properties of the PLA/PBAT blends and PLA/PBAT/clay systems.

Samples	Yield Strength	Yield Strain	Flexure Elast. Mod.
	(MPa)	(%)	(MPa)
1 PLA + PBAT pure blend	4.0 ± 1.0	1.8 ± 0.70	1248 ± 52.5
2 PLA + PBAT blend + 3% clay	15.5 ± 1.4	1.71 ± 0.20	1222 ± 37.2
3 PLA + PBAT blend + 6% clay	15.1 ± 0.3	1.75 ± 0.03	1263 ± 15.0
4 PBAT 3% clay concentrate + PLA	12.7 ± 1.0	1.42 ± 0.20	1443 ± 65.5
5 PBAT 6% clay concentrate + PLA	16.2 ± 2.0	2.00 ± 0.40	1388 ± 177
6 PLA 3% clay concentrate + PBAT	8.3 ± 0.5	1.00 ± 0.08	1249 ± 38.3
7 PLA 6% clay concentrate + PBAT	24.3 ± 1.8	1.46 ± 0.15	1485 ± 53.5
8 PLA + PBAT + 3% clay	11.7 ± 0.5	1.32 ± 0.06	1232 ± 45.6
9 PLA + PBAT + 6% clay	9.5 ± 2.0	1.14 ± 0.50	1224 ± 60.5

The reported data represents arithmetic mean values and the error bars refer to the standard deviation of the mean.

It is worth mentioning that the polymer chains that form the PBAT/PLA system exhibit a dipole moment as a function of the chain configuration (slight polarity difference), which most likely contributed to the increase of the properties. This finding can be confirmed when the mechanical performance obtained for the blend in sample 7 (PLA 6% clay concentrate + PBAT) is observed individually. Similar behavior was observed by Kumar et al.^[41] for PLA/PBAT/Glycidyl methacrylate nanocomposites with 5% clay, which exhibited a significant increase in the elastic modulus, in this case the additive plastificant (glycidyl) was essential to improve these properties because it provided better compatibility the matrices PLA/PBAT. This finding confirms that a change in the morphology of the system most likely occurred. When researching PLA/PBAT and acetyl tributyl citrate blends, Coltelli et al.^[48] showed that the plasticizer exhibited higher solubility in the PBAT phase because the dipole moment of this phase is on the order of 4132 Debye, while the dipole moment of the PLA is on the order of 3223 Debye.

The formation of the morphology of immiscible polymer blends is the result of interaction between process variables (temperature, deformation types and rate) and blend components properties (composition, viscosity ratio, interfacial tension, continuous phase viscosity and elasticity of the components). Thus, the final morphology is the combination of these factors. The initial particle size, the polymer elasticity, the dispersed phase percentage and the draw ratio are the main factors affecting the morphology formed during drawing. When the dispersed phase concentration gets close to 1:1, complex structures, such as ribbon- or sheet-like, platelet, stratified and continuous structures, are formed. However, the prevalence of one or other structure is basically controlled by factors such as the flow type and the intensity during its processing in the molten state, the viscosity ratio and the interfacial tension^[49-51].

Table 2 shows the results of the Izod impact strength tests for the PLA/PBAT blend and for the PLA/PBAT/clay systems. The results showed that the blending conditions and the increased clay concentration influenced the dispersion of the clay in the blends such that the samples with 6% clay had lower impact strengths regardless of the blending sequence. Nishida et al.^[52] showed that the addition of a crosslinking agent [5-Dimethyl 2,5-di(tert-butylperoxy)hexane] in the PLA/PBAT blend increased the fracture toughness of the Izod impact tests. Furthermore, it is important to highlight that polymer research has shown that the addition of conventional reinforcements can increase the stiffness of the material and simultaneously reduce the impact strength due to nucleating properties. This affects crystal growth and crystallization also acting as a stress concentrator. Defects that begin to form around the reinforcement will quickly create cracks that will cause fracturing or failure of the material. In general, studies have shown that the greatest challenge is to modify the stiffness of the PLA by adding more flexible polymers^[53]. The results of the mechanical properties of the PLA/PBAT/clay systems indicated the possibility of obtaining materials with good mechanical performance. A comparative analysis shows that it is possible to increase the mechanical properties (strength, tensile and bending elastic moduli, and impact strength) by adding organophilic clay to the PLA/PBAT system, a behavior similar to that found by Adrar et al.^[54].

3.2 X-Ray diffraction

Table 3 shows the interplanar basal distances for the PLA/PBAT/clay systems as well as the d_{001} values of the systems in relation to the d_{001} distance of the organophilic clay. Increases in the d_{001} interlamellar spacings were observed for all the systems, which indicates the formation of nanocomposites with intercalated structures. The largest values were for samples 4, 6 and 7. These results show that the different blending conditions influenced the polymer/clay interaction and consequently the degree of exfoliation of the clay in the polymer matrix. A similar behavior was found by Nofar et al.^[55], which analyzed blends of PLA with 25 wt% PBAT containing 1 and 5 wt% Cloisite 30B nanoclay that were prepared using an internal batch mixer with three mixing strategies. However, they conclude that this difference is not significant.

3.3 Scanning electron microscopy and transmission electron microscopy

SEM observations were performed for the morphological analyses of the PLA/PBAT/clay systems, and photomicrographs of the fracture surface of the specimens were obtained. These photomicrographs indicate that the blending sequence is directly responsible for the morphological changes in the bionanocomposites that formed. Possible clay clusters are observed in these photomicrographs (circled). Figures 2 to 6 show photomicrographs of the different PLA/PBAT/clay systems at concentrations of 3% and 6%.

Table 2. Impact properties of the PLA/PBAT blend and the PLA/PBAT/clay systems.

Samples	Izod Impact Strength
	(KJ/m ²)
1 PLA + PBAT pure blend	5.7 ± 0.5
2 PLA + PBAT blend + 3% clay	5.8 ± 0.2
3 PLA + PBAT blend + 6% clay	4.0 ± 0.3
4 PBAT 3% clay concentrate + PLA	6.5 ± 0.1
5 PBAT 6% clay concentrate + PLA	5.8 ± 0.2
6 PLA 3% clay concentrate + PBAT	4.8 ± 0.3
7 PLA 6% clay concentrate + PBAT	3.9 ± 0.2
8 PLA + PBAT + 3% clay	5.2 ± 0.2
9 PLA + PBAT + 6% clay	4.0 ± 0.1

The reported data represents arithmetic mean values and the error bars refer to the standard deviation of the mean.

Table 3. Interplanar basal distances for the PLA/PBAT/clay systems and the changes in the systems with organophilic clay.

System Evaluated	* d_{001} (Å)	** Δd (Å)
1 PLA + PBAT pure blend	-	-
2 PLA + PBAT blend + 3% clay	40.84	4.16
3 PLA + PBAT blend + 6% clay	41.86	5.18
4 PBAT 3% clay + PLA	45.04	8.36
5 PBAT 6% clay + PLA	39.05	2.37
6 PLA 3% clay + PBAT	45.04	8.36
7 PLA 6% clay + PBAT	42.84	6.16
8 PLA + PBAT + 3% clay	40.84	4.16
9 PLA + PBAT + 6% clay	42.40	5.72

* d_{001} of 1346 (OMMT) clay = 36.68(Å); ** Δd (Å) = changes in the interplanar basal distances (system - clay).

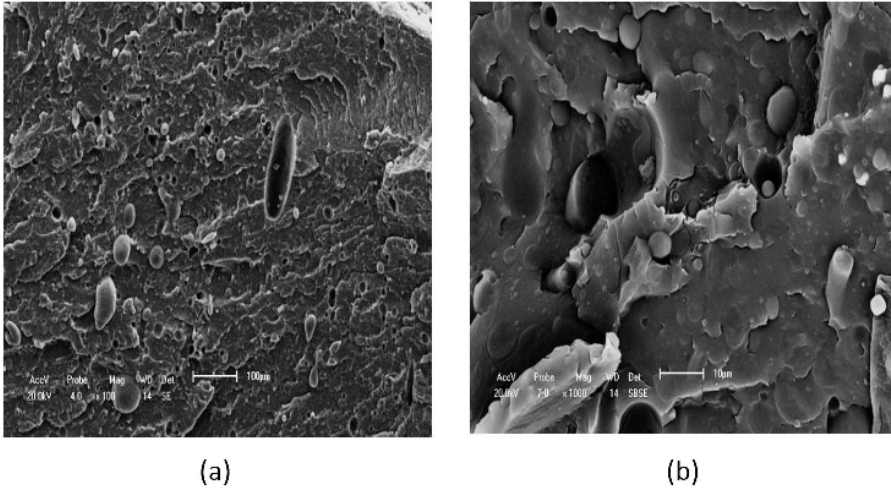


Figure 2. (a) SEM of the PLA/PBAT blend at 100X and (b) 1000X.

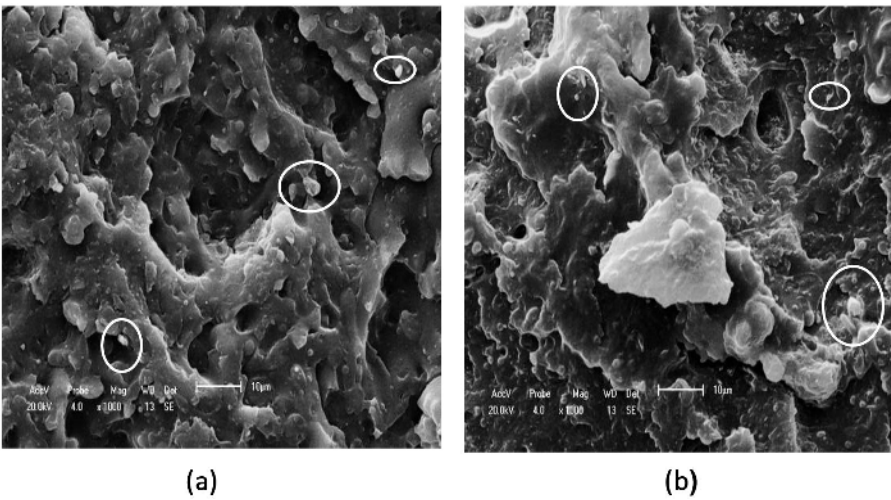


Figure 3. SEM at 1000X magnification of (a) PLA/PBAT blend + 3% clay and (b) PLA/PBAT blend + 6% clay.

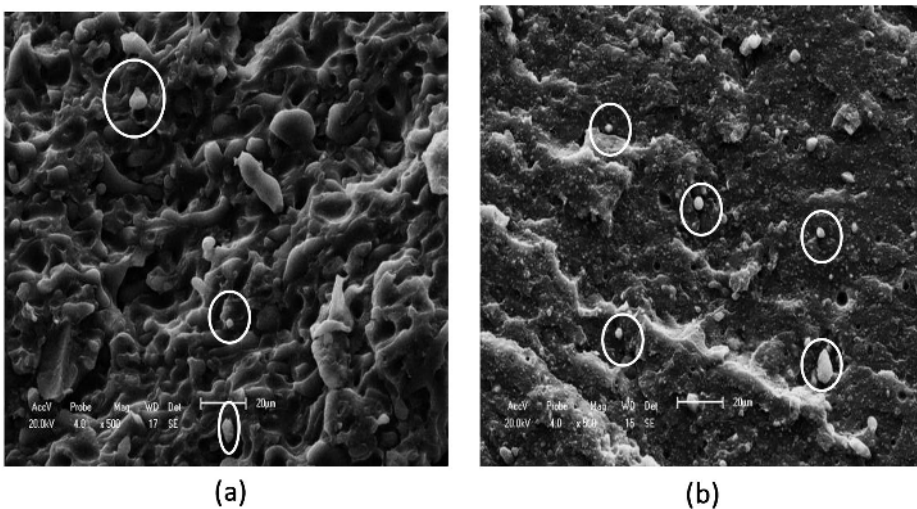


Figure 4. SEM at 500X magnification of (a) PBAT 3% clay concentration + PLA and (b) PBAT 6% clay concentration + PLA.

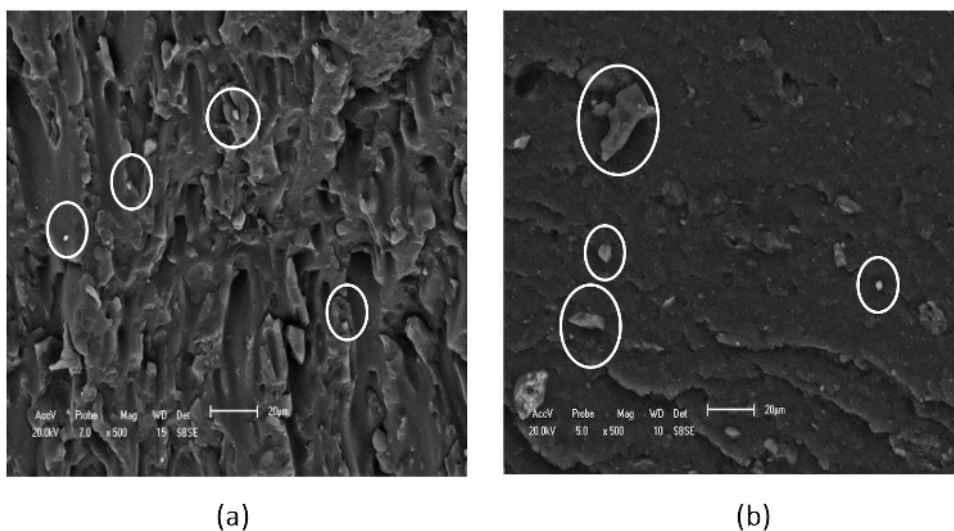


Figure 5. SEM at 500X magnification of (a) PLA 3% clay concentration + PBAT and (b) PLA 6% clay concentration + PBAT.

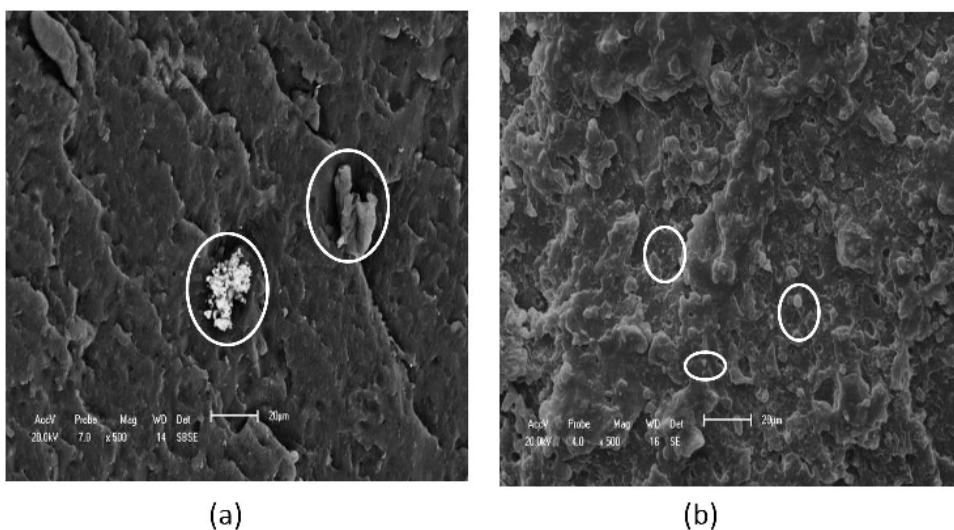


Figure 6. SEM at 500X magnification of (a) PLA + PBAT + 3% clay concentration and (b) PLA + PBAT + 6% clay concentration.

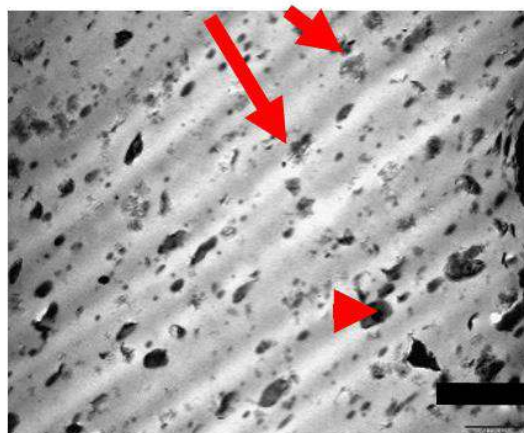
Figure 2 shows photomicrographs of the PLA/PBAT 50/50 blend. A distinct morphology is observed that is characteristic of an immiscible blend, where circular PBAT particles are dispersed in the PLA matrix. Kumar et al.^[41] and Zhang & Sun^[56] showed similar morphologies of blends composed of 70%PLA/30%PBAT. According to Zhang & Sun^[56], using glycidyl methacrylate as a compatibilizer resulted in better blend compatibility and dispersion.

The morphology of nanocomposites with intercalated and/or exfoliated structures cannot be observed by SEM; however, as a preliminary investigation, it is possible to evaluate the degree of dispersion of the clays. Therefore, the following photomicrographs present the morphologies of the PLA/PBAT/clay systems under different blending conditions as well as the degree of dispersion of the clays.

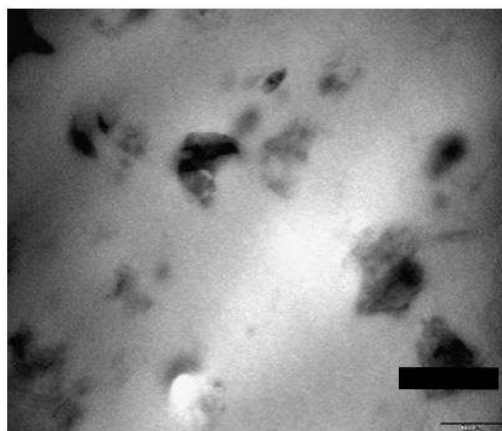
Freitas et al.^[57] demonstrated that PLA/PBAT blends containing MMT showed a dispersed phase covered by the matrix and Adrar et al.^[54] observed that fibrillar morphologies in the OMMT-PLA/PBAT blends. This morphology change may be an indication of an improvement of PLA/PBAT blending miscibility after the incorporation of OMMT.

Furthermore, the morphologies indicated that adding clay caused a change in the PLA and/or PBAT crystallization. Research by Xiao et al.^[58] on the kinetics of PLA crystallization showed that the PLA chain is sensitive to the presence of another phase and to the processing conditions. Therefore, we can conclude that adding clay disturbed the PLA/PBAT/clay system, which modified the growth of the spherulitic crystals and hindered the organization of the PLA chains.

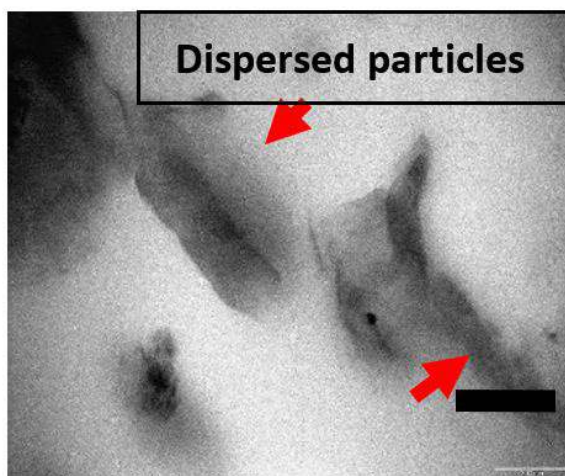
Tactoids (interspersed particles)



(a)



(b)



(c)

Figure 7. TEM of the PLA 6% clay concentrate + PBAT sample.

Correlating the results of the mechanical properties and the morphologies of the PLA/PBAT/clay systems showed that the higher values of the properties occurred in the samples that exhibited better PLA/PBAT/clay compatibility. For example, the morphology of sample 7 (PLA 6% clay concentrate + PBAT), which is shown in Figure 5b, shows the formation of a very dispersive PBAT phase and small clay clusters impregnated in the PBAT/PLA matrix, which caused its high mechanical performance.

Based on the mechanical properties, XRD and SEM properties of sample 7 (PLA 6% clay concentrate + PBAT) and taking into account the TEM data in Figure 7, good dispersion of the PBAT phase and the clay in the PLA matrix with partially intercalated regions was observed. This finding probably contributed to the good performance of these properties.

4. Conclusions

The current study investigated the influence of the different conditions blending (contend) 50%PLA/50%PBAT with 3 and 6% clay. In this study was prepared 8 samples PLA/PBAT/Clay bionanocomposites and analyzed mechanical properties and morphology. The addition of clay associated with the sequence used caused a change in the PLA/PBAT blends morphology, resulting in changes in the mechanical properties. Furthermore, the results transmission microscopy (TEM) to sample with PLA 6% clay concentrate + PBAT (sample 7) showed regions intercalated PBAT and clay in the PLA phase. The results may contribute to a better elucidation regarding the characteristics of the PLA/PBAT and OMMT blends, since the two polymers have gained great importance in the area of materials and with the addition of OMMT their properties can be improved.

5. Acknowledgements

The authors would like to thank the National Service for Industrial Training (Serviço Nacional de Aprendizagem Industrial) – SENAI (Bahia - Brazil), CNPq (Conselho Nacional de Desenvolvimento Científico e Tecnológico) and CAPES (Coordenação de Aperfeiçoamento de Pessoal de Nível Superior).

6. References

- Silva, J. B. A., Nascimento, T., Costa, L. A. S., Pereira, F. V., Machado, B. A. S., Gomes, G. V. P., Assis, D. J., & Druzian, J. I. (2015). Effect of source and interaction with nanocellulose cassava starch, glycerol and the properties of films bionanocomposites. *Materials Today*, 2(1), 200-207.
- Reis, L. C. B., Souza, C. O., Silva, J. B. A., Martins, A. C., Nunes, I. L., & Druzian, J. I. (2015). Active biocomposites of cassava starch: the effect of yerba mate extract and mango pulp as antioxidant additives on the properties and the stability of a packaged product. *Food and Bioprocess Processing*, 94, 382-391. <http://dx.doi.org/10.1016/j.fbp.2014.05.004>.
- Lin, X., Fan, X., Li, R., Li, Z., Ren, T., Ren, X., & Huang, T. S. (2018). Preparation and characterization of PHB/PBAT-based biodegradable antibacterial hydrophobic nanofibrous membranes. *Polymers for Advanced Technologies*, 29(1), 481-489. <http://dx.doi.org/10.1002/pat.4137>.
- Brockhaus, S., Petersen, M., & Kersten, W. (2016). A crossroads for bioplastics: exploring product developers' challenges to move beyond petroleum-based plastics. *Journal of Cleaner Production*, 127, 84-95. <http://dx.doi.org/10.1016/j.jclepro.2016.04.003>.
- Emadian, S. M., Onay, T. T., & Demirel, B. (2017). Biodegradation of bioplastics in natural environments. *Waste Management (New York, N.Y.)*, 59, 526-536. <http://dx.doi.org/10.1016/j.wasman.2016.10.006>. PMID:27742230.
- Tang, X. Z., Kumar, P., Alavi, S., & Sandeep, K. P. (2012). Recent advances in biopolymers and biopolymer-based nanocomposites for food packaging materials. *Critical Reviews in Food Science and Nutrition*, 52(5), 426-442. <http://dx.doi.org/10.1080/10408398.2010.500508>. PMID:22369261.
- Brito, G. F., Agrawal, P., Araújo, E. M., & Mélo, T. J. A. (2012). Polylactide/biopolyethylene bioblends. *Polímeros: Ciência e Tecnologia*, 22(5), 427-429. <http://dx.doi.org/10.1590/S0104-14282012005000072>.
- Machado, B. A. S., Reis, J. H. O., Silva, J. B., Cruz, L. S., Nunes, I. L., Vargas, F. P., & Druzian, J. I. (2014). Obtenção de nanocelulose da fibra de coco verde e incorporação em filmes biodegradáveis de amido plastificados com glicerol. *Química Nova*, 37, 1-8.
- Machado, B. A. S., Silva, J. B., & Druzian, J. I. (2010). *Patent No 011100001122*. Rio de Janeiro: Instituto Nacional da Propriedade Industrial – INPI.
- Selígra, P. G., Jaramillo, C. M., Famá, L., & Goyanes, S. (2016). Biodegradable and non-retrogradable eco-films based on starch-glycerol with citric acid as crosslinking agent. *Carbohydrate Polymers*, 138(1), 66-74. <http://dx.doi.org/10.1016/j.carbpol.2015.11.041>. PMID:26794739.
- Venkatesan, R., & Rajeswari, N. (2016). ZnO/PBAT nanocomposite films: investigation on the mechanical and biological activity for food packaging. *Polymers for Advanced Technologies*, 28(1), 20-27. <http://dx.doi.org/10.1002/pat.3847>.
- Arrieta, M. P., Samper, M. D., Aldas, M., & López, J. (2017). On the use of PLA-PHB blends for sustainable food packaging applications. *Materials (Basel)*, 10(9), 1-26. <http://dx.doi.org/10.3390/ma10091008>.
- Perazzo, K. K. N. C. L., Conceição, A. C. V., Santos, J. C. P., Assis, D. J., Souza, C. O., & Druzian, J. I. (2014). Properties and antioxidant action of actives cassava starch films incorporated with green tea and palm oil extracts. *PLoS One*, 9(9), e105199. <http://dx.doi.org/10.1371/journal.pone.0105199>. PMID:25251437.
- Machado, B. A. S., Nunes, I. L., Pereira, F. V., & Druzian, J. I. (2012). Desenvolvimento e avaliação da eficácia de filmes biodegradáveis de amido de mandioca com nanocelulose como reforço e com extrato de erva-mate como aditivo antioxidante. *Ciência Rural*, 42(11), 2085-2091. <http://dx.doi.org/10.1590/S0103-84782012001100028>.
- Correa, J. P., Molina, V., Sanchez, M., Kainz, C., Eisenberg, P., & Massani, M. B. (2017). Improving ham shelf life with a polyhydroxybutyrate/polycaprolactone biodegradable film activated with nisin. *Food Packaging and Shelf Life*, 11, 31-39. <http://dx.doi.org/10.1016/j.fpsl.2016.11.004>.
- Shankar, S., & Rhim, J. W. (2016). Preparation of nanocellulose from micro-crystalline cellulose: the effect on the performance and properties of agar-based composite films. *Carbohydrate Polymers*, 135, 18-26. <http://dx.doi.org/10.1016/j.carbpol.2015.08.082>. PMID:26453846.
- Stanzione, M., Gargiulo, N., Caputo, D., Liguori, B., Cerruti, P., Amendola, E., Lavorgna, M., & Buonocore, G. G. (2017). Peculiarities of vanillin release from amino-functionalized mesoporous silica embedded into biodegradable composites. *European Polymer Journal*, 89, 88-100. <http://dx.doi.org/10.1016/j.eurpolymj.2017.01.040>.
- Varaprasad, K., Pariguana, M., Raghavendra, G. M., Jayaramudu, T., & Sadiku, E. R. (2017). Development of biodegradable metaloxide/polymer nanocomposite films based on poly-ε-caprolactone and terephthalic acid. *Materials Science and Engineering C*, 70(Pt 1), 85-93. <http://dx.doi.org/10.1016/j.msec.2016.08.053>. PMID:27770963.
- Marvdashti, L. M., Koocheki, A., & Yavarmanesh, M. (2017). Alyssum homolecarpum seed gum-polyvinyl alcohol biodegradable composite film: Physicochemical, mechanical, thermal and barrier properties. *Carbohydrate Polymers*, 155, 280-293. <http://dx.doi.org/10.1016/j.carbpol.2016.07.123>. PMID:27702514.
- Altomare, L., Bonetti, L., Campiglio, C. E., De Nardo, L., Draghi, L., Tana, F., & Faré, S. (2018). Biopolymer-based strategies in the design of smart medical devices and artificial organs. *The International Journal of Artificial Organs*, 41(6), 337-359. <http://dx.doi.org/10.1177/0391398818765323>. PMID:29614899.
- Smith, R. (2005). *Biodegradable polymers for industrial applications*. Boca Raton: Woodhead Publishing Limited and CRC Press LLC.
- Touchaleaume, F., Martin-Closas, L., Angellier-Coussy, H., Chevillard, A., Cesar, G., Gontard, N., & Gastaldi, E. (2016). Performance and environmental impact of biodegradable polymers as agricultural mulching films. *Chemosphere*, 144, 433-439. <http://dx.doi.org/10.1016/j.chemosphere.2015.09.006>. PMID:26386433.
- Basko, M., Bednarek, M., Vlaminck, L., Kubisa, P., & Du Prez, F. E. (2017). Biodegradable polymer networks via triazolinedione-crosslinking of oleyl-functionalized poly(ε-caprolactone). *European Polymer Journal*, 89, 230-240. <http://dx.doi.org/10.1016/j.eurpolymj.2017.02.031>.
- Shahbazi, M., Rajabzadeh, G., Rafe, A., Ettelaie, R., & Ahmadi, S. J. (2016). The physico-mechanical and structural characteristics of blend film of poly (vinyl alcohol) with biodegradable polymers as affected by disorder-to-order conformational transition. *Food Hydrocolloids*, 60, 393-404. <http://dx.doi.org/10.1016/j.foodhyd.2016.03.038>.

25. Pivsa-Art, W., Chaiyasat, A., Pivsa-Art, S., Yamane, H., & Ohara, H. (2013). Preparation of polymer blends between poly(lactic acid) and poly(butylene adipate-co-terephthalate) and biodegradable polymers as compatibilizers. *Energy Procedia*, 34, 549-554. <http://dx.doi.org/10.1016/j.egypro.2013.06.784>.
26. Garavand, F., Rouhi, M., Razavi, S. H., Cacciotti, I., & Mohammadi, R. (2017). Improving the integrity of natural biopolymer films used in food packaging by crosslinking approach: a review. *International Journal of Biological Macromolecules*, 104(Pt A), 687-707. <http://dx.doi.org/10.1016/j.ijbiomac.2017.06.093>. PMID:28652152.
27. Doppalapudi, S., Jain, A., Khan, W., & Domb, A. J. (2014). Biodegradable polymers-an overview. *Polymers for Advanced Technologies*, 25(5), 427-435. <http://dx.doi.org/10.1002/pat.3305>.
28. Dhandapani, S., Nayak, S. K., & Mohanty, S. (2016). Analysis and evaluation of biobased polyester of PTT/PBAT blend: thermal, dynamic mechanical, interfacial bonding, and morphological properties. *Polymers for Advanced Technologies*, 27(7), 938-945. <http://dx.doi.org/10.1002/pat.3752>.
29. Wei, L., & McDonald, A. G. (2016). A review on grafting of biofibers for biocomposites. *Materials (Basel)*, 9(4), 1-23. <http://dx.doi.org/10.3390/ma9040303>. PMID:28773429.
30. Weng, Y. X., Jin, Y. J., Meng, Q. Y., Wang, L., Zhang, M., & Wang, Y. Z. (2013). Biodegradation behavior of poly(butylene adipate-co-terephthalate) (PBAT), poly(lactic acid) (PLA), and their blend under soil conditions. *Polymer Testing*, 32(5), 918-926. <http://dx.doi.org/10.1016/j.polymertesting.2013.05.001>.
31. Karamanlioglu, M., Preziosi, R., & Robson, G. D. (2017). Abiotic and biotic environmental degradation of the bioplastic polymer poly(lactic acid): a review. *Polymer Degradation & Stability*, 137, 122-130. <http://dx.doi.org/10.1016/j.polymdegradstab.2017.01.009>.
32. Finzi-Quintão, C. M., Novack, K. M., Bernardes-Silva, A. C., Silva, T. D., Moreira, L. E. S., & Braga, L. E. M. (2018). Influence of Moringa oleifera derivatives in blends of PBAT/PLA with LDPE. *Polímeros: Ciência e Tecnologia*, 28(4), 309-318. <http://dx.doi.org/10.1590/0104-1428.05717>.
33. Paul, D. R., & Robeson, L. M. (2008). Polymer nanotechnology: nanocomposites. *Polymer*, 49(15), 3187-3204. <http://dx.doi.org/10.1016/j.polymer.2008.04.017>.
34. Nofar, M., Heuzey, M. C., Carreau, P. J., & Kamal, M. R. (2016). Effects of nanoclay and its localization on the morphology stabilization of PLA/PBAT blends under shear flow. *Polymer*, 98, 353-364. <http://dx.doi.org/10.1016/j.polymer.2016.06.044>.
35. Wu, N., & Zhang, H. (2017). Mechanical properties and phase morphology of super-tough PLA/PBAT/EMA-GMA multicomponent blends. *Materials Letters*, 192, 17-20. <http://dx.doi.org/10.1016/j.matlet.2017.01.063>.
36. Ojijo, V., & Ray, S. S. (2014). Nano-biocomposites based on synthetic aliphatic polyesters and nanoclay. *Progress in Materials Science*, 62, 1-57. <http://dx.doi.org/10.1016/j.pmatsci.2014.01.001>.
37. Kornmann, X. (1999). *Synthesis and characterisation of thermoset-clay nanocomposites* (Licentiate dissertation). Luleå Tekniska Universite, Luleå.
38. Ferreira, L. P., Moreira, A. N., Souza, F. G. Jr, & Pinto, J. C. C. S. (2014). Preparo de nanocompósitos de Poli(Succinato de Butileno) (PBS) e argila motmorilonita organofílica via polimerização *in situ*. *Polímeros: Ciência e Tecnologia*, 24(5), 604-611. <http://dx.doi.org/10.1590/0104-1428.1662>.
39. Zare, Y. (2016). Effects of imperfect interfacial adhesion between polymer and nanoparticles on the tensile modulus of clay/polymernanocomposites. *Applied Clay Science*, 129, 65-70. <http://dx.doi.org/10.1016/j.clay.2016.05.002>.
40. Zare, Y. (2017). An approach to study the roles of percolation threshold and interphase in tensile modulus of polymer/claynanocomposites. *Journal of Colloid and Interface Science*, 486, 249-254. <http://dx.doi.org/10.1016/j.jcis.2016.09.080>. PMID:27721073.
41. Kumar, M., Mohanty, S., Nayak, S. K., & Rahail-Parvaiz, R. (2010). Effect of glycidyl Methacrylate (GMA) on the thermal, mechanical and morphological property of biodegradable PLA/PBAT blend and its nanocompositos. *Bioresource Technology*, 101(21), 8406-8415. <http://dx.doi.org/10.1016/j.biortech.2010.05.075>. PMID:20573502.
42. Zhang, N., Wang, Q., Ren, J., & Wang, L. (2009). Preparation and properties of biodegradable poly(lactic acid)/poly(butylene adipate-co-terephthalate) blend with glycidyl methacrylate as reactive processing agent. *Journal of Materials Science*, 44(1), 250-256. <http://dx.doi.org/10.1007/s10853-008-3049-4>.
43. Barbosa, R. (2009). *Study of the modification of bentonite clays for application in polyethylene nanocomposites* (Doctoral thesis). Universidade Federal de Campina Grande, Campina Grande.
44. Rodrigues, A. W. B. (2009). *Organophilization of bentonite clays and application in the development of nanocomposites with polypropylene matrix* (Doctoral thesis). Universidade Federal de Campina Grande, Campina Grande.
45. Signori, F., Coltelli, M. B., & Bronco, S. (2009). Thermal degradation of poly(lactic acid) (PLA) and poly(butylene adipate-co-terephthalate) (PBAT) and their blends upon melt processing. *Polymer Degradation & Stability*, 94(1), 74-82. <http://dx.doi.org/10.1016/j.polymdegradstab.2008.10.004>.
46. Jiang, L., Wolcott, M. P., & Zhang, J. (2006). Study of biodegradable polylactide/poly(butylene adipate-co-terephthalate) blends. *Biomacromolecules*, 7(1), 199-207. <http://dx.doi.org/10.1021/bm050581q>. PMID:16398516.
47. Ko, S. W., Hong, M. K., Park, B. J., Gupta, R. K., Choi, H. J., & Bhattacharya, S. N. (2009). Morphological and rheological characterization of multiwalled carbon nanotube/PLA/PBAT blend nanocomposites. *Polymer Bulletin*, 63(1), 125-134. <http://dx.doi.org/10.1007/s00289-009-0072-9>.
48. Coltelli, M.-B., Maggiore, I. D., Bertoldo, M., Signori, F., Bronco, S., & Ciardelli, F. (2008). Poly(lactic acid) properties as a consequence of poly(butylene adipate-co-terephthalate) blending and acetyl tributyl citrate plasticization. *Journal of Applied Polymer Science*, 110(2), 1250-1262. <http://dx.doi.org/10.1002/app.28512>.
49. Ebnesaajjad, S. (2012). *Plastic films in food packaging: materials, technology and applications*. Amsterdam: Elsevier.
50. Viana, J. D., Araújo, E. M., & Melo, T. J. A. (2012). Evaluation of mechanical and morphological properties of bionanocomposites PLA/PBAT/organophilic clay. *Revista Eletrônica de Materiais e Processos*, 7, 20-25.
51. Arruda, L. C., Magaton, M., Bretas, R. E. S., & Ueki, M. M. (2015). Influence of chain extender on mechanical, thermal and morphological properties of blown films of PLA/PBAT blends. *Polymer Testing*, 43, 27-37. <http://dx.doi.org/10.1016/j.polymertesting.2015.02.005>.
52. Nishida, M., Ichihara, H., Watanabe, H., Fukuda, N., & Ito, H. (2015). Improvement of dynamic tensile properties of Poly(lactic acid)/Poly(butylene adipate-co-terephthalate) polymer alloys using a crosslinking agent and observation of fracture surfaces. *International Journal of Impact Engineering*, 79, 117-125. <http://dx.doi.org/10.1016/j.ijimpeng.2014.11.010>.
53. Liu, D., Li, H., Zhou, G., Yuan, M., & Qin, Y. (2015). Biodegradable poly(lactic-acid)/poly(trimethylene-carbonate)/laponite composite film: development and application to the packaging of mushrooms (*Agaricus bisporus*). *Polymers for*

- Advanced Technologies*, 26(12), 1600-1607. <http://dx.doi.org/10.1002/pat.3587>.
54. Adrar, S., Habi, A., Ajjji, A., & Grohens, Y. (2018). Synergistic effects in epoxy functionalized graphene and modified organo-montmorillonite PLA/PBAT blends. *Applied Clay Science*, 157, 65-75. <http://dx.doi.org/10.1016/j.clay.2018.02.028>.
55. Nofar, M., Heuzey, M. C., Carreau, P. J., & Kamal, M. R. (2016). Effects of nanoclay and its localization on the morphology stabilization of PLA/PBAT blends under shear flow. *Polymer*, 98, 353-364. <http://dx.doi.org/10.1016/j.polymer.2016.06.044>.
56. Zhang, J. F., & Sun, X. (2004). Mechanical properties of poly(lactic acid)/starch composites compatibilized by maleic anhydride. *Biomacromolecules*, 5(4), 1446-1451. <http://dx.doi.org/10.1021/bm0400022>. PMID:15244463.
57. Freitas, A. L. P. L., Tonini, L. R. Fo., Calvão, P. S., & Souza, A. M. C. (2017). Effect of montmorillonite and chain extender on rheological, morphological and biodegradation behavior of PLA/PBAT blends. *Polymer Testing*, 62, 189-195. <http://dx.doi.org/10.1016/j.polymertesting.2017.06.030>.
58. Xiao, H., Lu, W., & Yeh, J. T. (2009). Crystallization behavior of fully biodegradable poly(lactic acid)/poly(butylene adipate-co-terephthalate) blends. *Journal of Applied Polymer Science*, 112(6), 3754-3763. <http://dx.doi.org/10.1002/app.29800>.

Received: Jan. 29, 2019

Revised: Aug. 28, 2019

Accepted: Sept. 21, 2019